

# REPORTS

*Ecology*, 87(3), 2006, pp. 535–541  
© 2006 by the Ecological Society of America

## FUNDAMENTAL TRADE-OFFS GENERATING THE WORLDWIDE LEAF ECONOMICS SPECTRUM

BILL SHIPLEY,<sup>1,5</sup> MARTIN J. LECHOWICZ,<sup>2</sup> IAN WRIGHT,<sup>3</sup> AND PETER B. REICH<sup>4</sup>

<sup>1</sup>*Département de biologie, Université de Sherbrooke, Sherbrooke, Quebec J1K 2R1 Canada*

<sup>2</sup>*Department of Biology, McGill University, 1205 Avenue Dr. Penfield, Montreal, Quebec H3A 1B1 Canada*

<sup>3</sup>*Macquarie University, Department of Biological Sciences, Sydney 2109 Australia*

<sup>4</sup>*Department of Forest Resources, University of Minnesota, 1530 Cleveland Avenue North, St. Paul, Minnesota 55108 USA*

**Abstract.** Recent work has identified a worldwide “economic” spectrum of correlated leaf traits that affects global patterns of nutrient cycling and primary productivity and that is used to calibrate vegetation–climate models. The correlation patterns are displayed by species from the arctic to the tropics and are largely independent of growth form or phylogeny. This generality suggests that unidentified fundamental constraints control the return of photosynthates on investments of nutrients and dry mass in leaves. Using novel graph theoretic methods and structural equation modeling, we show that the relationships among these variables can best be explained by assuming (1) a necessary trade-off between allocation to structural tissues versus liquid phase processes and (2) an evolutionary trade-off between leaf photosynthetic rates, construction costs, and leaf longevity.

**Key words:** comparative ecology; leaf life span; leaf longevity; leaf mass per area, LMA; leaf nitrogen content; net photosynthetic rate; path analysis; specific leaf area, SLA; structural equations modeling, SEM; vanishing tetrads.

### INTRODUCTION

The results of natural selection in diverse environments, contingent on various physiochemical and phylogenetic constraints, are mirrored in the multivariate patterns of correlation among heritable traits of functional significance. Consider leaf form and function. Given the incredible variation in leaf form and physiological performance, given the deep phylogenetic origin of this variation, and given the wide variety of environments in which leaves operate, one might expect many different types of trade-offs involving leaf form and function. If so, then the patterns of correlation among functional leaf traits should vary greatly across differing phylogenies and environments. This expectation is contradicted by nature (Reich et al. 1997, Wright et al. 2004). A single principal component captures 74% of the total variance in six key foliar traits in the GLOPNET data set (Wright et al. 2004) which involves 2548 species from 219 families representing 175 sites from the arctic to the tropics. Fully 82% of the variation in the four variables of interest in the present paper (maximum photosynthetic rate, leaf mass

per area, leaf life span, and nitrogen content per mass) is captured by a single principal component.

Why does this suite of leaf traits correlate so strongly in such different species and environments? Wright et al. (2004) suggest that it “reflects a mixture of direct and indirect causal relationships between traits,” but what is the nature of such relationships? It is not possible to answer this question in an interspecific context through experimental manipulation. One cannot, for example, either randomly assign, or directly manipulate, values of leaf mass per area (LMA) to widely different species independently of their other leaf attributes. An alternative approach, made possible by the marriage of confirmatory structural equations modeling and recent advances linking the structure of directed acyclic graphs with probability distributions, is to derive the predicted patterns of trait covariation implied in different hypothetical causal processes and statistically compare these to the empirical patterns.

Here, we adopt this novel approach to study the relationships among four key leaf attributes in the GLOPNET data set: maximum photosynthetic rate ( $A_m$ ), leaf mass per area (LMA), nitrogen content per mass ( $N_m$ ), and leaf longevity (LL). We first test two alternative path models that have been proposed in the literature. We then apply two new exploratory algorithms based on directed acyclic graphs to discover the correlational

Manuscript received 18 July 2005; revised 4 October 2005; accepted 5 October 2005. Corresponding Editor: A. M. Ellison.

<sup>5</sup> E-mail: Bill.Shipley@USherbrooke.ca

constraints on inter-relationships among traits that exist in these data and, using these results, develop a new hypothesis to explain the worldwide leaf economics spectrum. Finally, we test this hypothesis using structural equations modeling.

#### METHODS AND MATERIALS

The GLOPNET data set contains 2496 observations on 2020 different species, including 492 species for which data were available for all four variables, the rest having missing values for at least one of the four. The combination  $A_m$ –LL had the fewest observations (511) and the average number of observations per variable pair was 1128 (the complete data set is *available online*).<sup>6</sup> To assure homogeneity of variance and linearity, all observed variables were transformed to their natural logarithms. Structural equation models were fit using the MPLUS program (Muthén and Muthén 1998–2001) by maximizing the likelihood conditional on the structural constraints implied by the model when comparing the model and the empirical covariance matrices. Further details are found in the Appendix. Following Little and Rubin (1987), we assumed that missing values were “missing at random,” which is consistent with the diverse decisions on what to measure made by the many investigators whose results appear in the compiled data. Other assumptions of the likelihood test are approximate multivariate normality and linearity in the trends between the variables after data transformation. Judging from normal quantile plots, we believe that the data satisfy both assumptions.

Vanishing tetrads were evaluated using the TETRAD program and tested using Wishart’s asymptotic derivation for the sampling variance (Wishart 1928). The exploratory path analysis assuming no latent variables was done using the EPA2 program. Both programs are described in Shipley (2000a:306). Details of the tetrad representation theorem and the algorithm for exploratory path analysis are given in the Appendix.

#### RESULTS

##### Testing pre-existing structural hypotheses

We identified two different explanations in the literature for the patterns of covariation among these traits (Fig. 1). Fig. 1a is taken from the interpretation given by Wright et al. (2004): “. . . the linkage of high  $A_m$  with high  $N_m$  is in large part the result of a direct causal relationship (Field and Mooney 1986) (i.e.,  $N_m \rightarrow A_m$ ). Similarly, long LL requires the robustness and low palatability (including chemical defenses) associated with high LMA (i.e.,  $LMA \rightarrow LL$ ). More indirectly, high  $A_m$  tends to be associated with short LL because it requires high  $N_m$  and/or low LMA (i.e.,  $LMA \leftrightarrow N_m$ ), which increase leaf vulnerability to herbivory and physical hazards, and because high  $A_m$  drives fast

<sup>6</sup> <http://www.nature.com/nature/journal/v428/n6985/supinfo/nature02403.html>

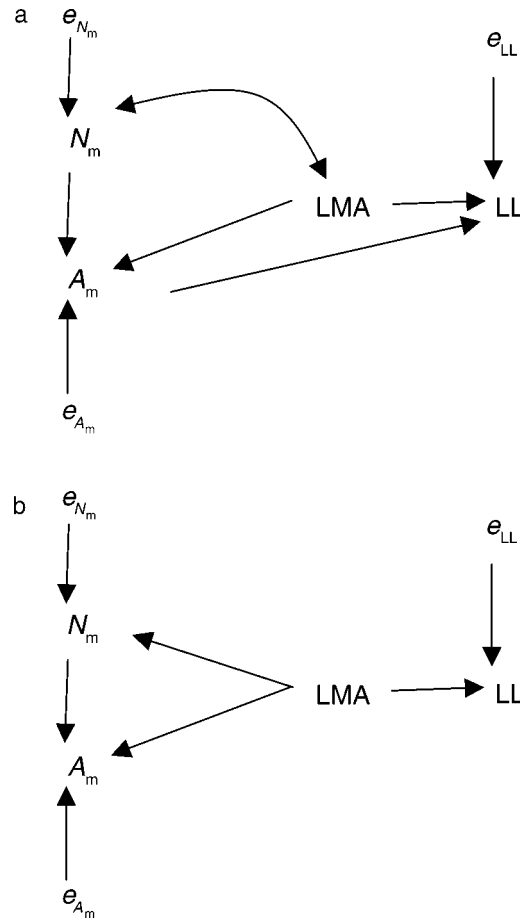


FIG. 1. Directed acyclic graphs of two competing models in the literature proposed to explain the interspecific patterns of covariation among leaf mass per area (LMA), maximum leaf photosynthetic rate on a mass basis ( $A_m$ ), leaf life span (LL), and leaf nitrogen concentration per dry mass ( $N_m$ ). Error variances ( $e$ ) are also shown. Both models are rejected at a probability below  $3 \times 10^{-4}$ .

growth, rapidly shading older leaves, leading them to senesce once their resources become more valuable when transferred to better-lit newer foliage (i.e.,  $A_m \rightarrow LL$ .” The second explanation (Fig. 1b, involving  $A_m$ ,  $N_m$ , and LMA) is based on the path model of Meziane and Shipley (2001) plus the preceding expectation involving LL. Using structural equation modeling, we tested both models representing the hypothesized causal origins of the functional relationships among the traits. Both models were unequivocally rejected (model 1a,  $\chi^2 = 12.825$ ,  $df = 1$ ,  $P = 0.0003$ ; model 1b,  $\chi^2 = 209.37$ ,  $df = 2$ ,  $P < 1 \times 10^{-15}$ ), suggesting that they do not adequately explain the covariation among these traits.

Although many additional models are conceivable, is there any testable ordering of the four variables that fits the data without invoking any additional variables influencing the patterns of correlation? If such an ordering exists, then there will be at least one path model

with positive degrees of freedom that fits the data (Shipley 2000a). We used the CI (Pearl 2000) and FCI (Spirites et al. 2000) algorithms, which provide an exhaustive search over the space of potential orderings, to obtain potential path models with positive degrees of freedom that then were each tested using the d-sep test of Shipley (2000b, 2003) at a significance level of  $P = 0.05$  and using Pearson (partial) correlation coefficients; details of these tests are in the Appendix. This search was based only on the 492 observations for which all four variables were measured. No such fitting model was found. This is strong statistical evidence that the interspecific patterns of correlation among these four leaf traits are generated by one or more variables not considered in this initial analysis (i.e., latent variables). Even stronger statistical evidence for the influence of latent variables is obtained using the tetrad representation theorem, which specifies the necessary and sufficient conditions for detecting the influence of at least one unmeasured (latent) variable on the relationships among measured variables. Of the three possible tetrad equations involving the four measured leaf traits in our analyses, only one tetrad equation is not significantly different from zero:

$$\rho_{\ln(LL), \ln(N_m)} \rho_{\ln(LMA), \ln(A_m)} = \rho_{\ln(LL), \ln(LMA)} \rho_{\ln(N_m), \ln(A_m)}$$

( $z = 1.404$ ,  $P = 0.16$ ), and there is only one pair of measured variables ( $A_m$  and LL) common to the two nonzero tetrads. This means that all causal paths linking every pair of variables except for LL and  $A_m$  pass through the same latent variable.

*A new hypothesis for the worldwide leaf economics spectrum*

Given this evidence for a latent variable, we propose an alternate explanation for the patterns of correlation among the four measured foliar traits that involves (1) unmeasured variation in cell size and cell wall thickness and (2) selection on leaf longevity to maximize plant carbon gain rather than leaf-level carbon gain.

*Variation in cell size and cell wall thickness.*—We divide the volume of a leaf ( $V_L$ ) into three compartments: the volume occupied by air spaces ( $V_a$ ), the volume occupied by cell walls ( $V_w$ ), and the volume bounded by the cell membranes of living cells ( $V_c$ ). This third compartment consists mostly of liquid. Here, the cell wall is not included in the cell volume. This is a slight modification of the model of Roderick (Roderick et al. 1999a, b). The ratio  $V_c/V_w$  is determined by the average size of a living cell in the leaf relative to the thickness of the average cell wall.

*Nitrogen per dry mass.*—Leaf nitrogen is found primarily within the cell, not in the cell wall (Hikosaka 2004). Let the average mass of nitrogen per cell volume be  $\bar{n}$ . The total mass of nitrogen per leaf ( $N$ ) is therefore  $N \cong \bar{n}V_c$  with strict equality if all nitrogen is in the cell. Let the average density of the tissue mass be  $d$ . The amount of nitrogen per dry mass ( $N_m$ ) in a leaf

with a tissue mass ( $M_t$ ) that is found both within the cell ( $M_c$ ) and in the cell wall ( $M_w$ ) is

$$N_m = \frac{N}{M_c + M_w} \cong \frac{\bar{n}V_c}{M_c + M_w}$$

If the cell does not contain large quantities of nonstructural carbohydrates then

$$M_w \gg M_c \quad N_m \cong \frac{\bar{n}V_c}{dV_w}$$

where  $d$  (specific gravity) is relatively constant among species at 1.5 (Desch 1973). Since nitrogen per liquid volume is only half as variable as  $N_m$  across species (Roderick et al. 1999b),  $\bar{n}$  will be even less variable, implying that most of the interspecific variation in  $N_m$  is due to variation in cell size vs. cell wall thickness (i.e.,  $V_c/V_w \rightarrow N_m$ ).

*Net photosynthesis per dry mass.*—Carbon fixation in the Calvin cycle occurs within the lumen (liquid phase) of the chloroplast. Furthermore, chloroplast number per cell increases with cell size in interspecific comparisons (Pyankov et al. 1999, Pyke 1999). Therefore, if  $\bar{a}$  is the average rate of net carbon fixation per cell volume and  $A$  is the total net carbon fixation per leaf, then the rate of net photosynthesis per dry mass ( $A_m$ ) is

$$A_m = \frac{A}{M_c + M_w} \cong \frac{\bar{a}V_c}{dV_w}$$

(i.e.,  $V_c/V_w \rightarrow A_m$ ).

*Leaf mass per area (LMA).*—For simplicity, we start with specific leaf area (SLA) and note that  $LMA = SLA^{-1}$ . Since the total volume of a leaf ( $V_L$ ) is the product of projected leaf surface area ( $S$ ) and the average leaf thickness ( $T$ ),

$$SLA = \frac{S}{M_c + M_w} = \frac{V_L}{T(M_c + M_w)} \cong \frac{V_L}{T(dV_w)}$$

Therefore,

$$SLA \cong \frac{V_c + V_w + V_a}{T(dV_w)} = \frac{1}{d} \left( \frac{V_c}{TV_w} + \frac{1}{T} + \frac{V_a}{V_w} \right)$$

and LMA will respond in the same way but with opposite signs; i.e., it will decrease with an increasing ratio  $V_c/V_w$  (i.e.,  $V_c/V_w \rightarrow LMA$ ).

*Optimal leaf longevity.*—Kikuzawa's (1991) model predicts that if natural selection optimizes plant carbon fixation per unit time over the life of a leaf, then the optimal leaf longevity should increase with decreasing maximum net photosynthetic rate of the leaf once expansion has terminated (i.e.,  $LL \rightarrow A_m$ ), and should increase with increasing leaf construction cost (i.e.,  $CC \rightarrow A_m$ ). The construction cost is the total amount of resources (ultimately energy) that the plant must invest to construct the leaf. Let the construction cost (usually quantified in terms of glucose-equivalents expended) needed to absorb, fix, transport or biochemically ma-

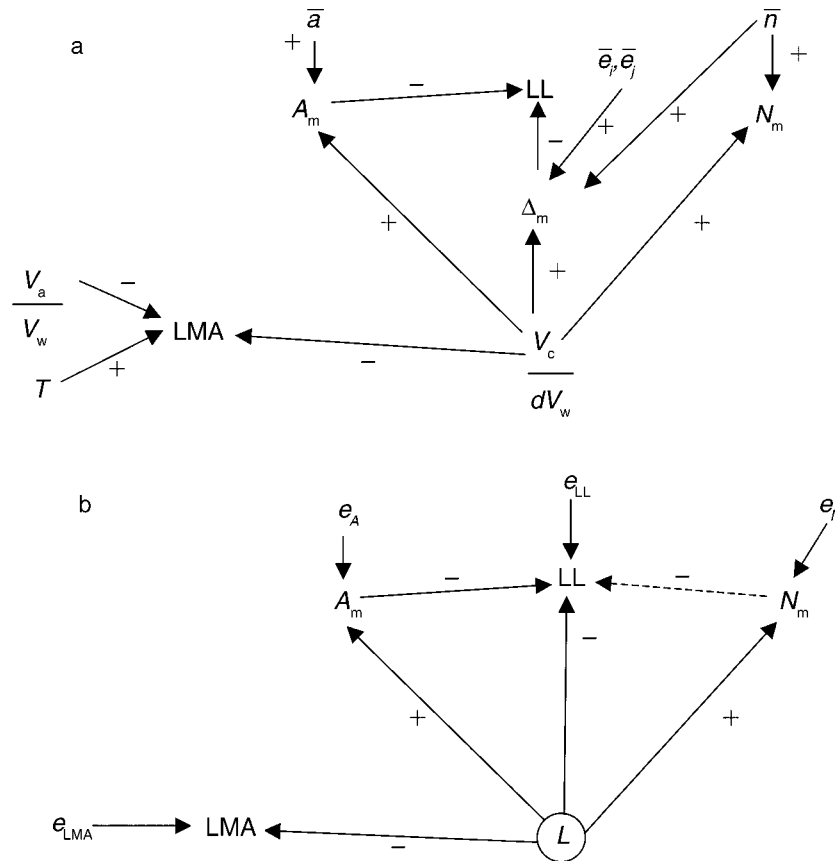


FIG. 2. (a) Theoretical relationships between the observed variables in Fig. 1 and unmeasured variables (volumes of the cell [ $V_c$ ], the cell wall [ $V_w$ ], and air spaces [ $V_a$ ], lamina thickness [ $T$ ], mass density of the cell wall [ $d$ ], average mass of nitrogen [ $\bar{n}$ ], other elements within the cell [ $\bar{e}_i$ ] per cell volume, average mass of elements within the cell wall per cell volume [ $\bar{e}_j$ ], average rate of net carbon fixation per cell volume [ $\bar{a}$ ], and construction cost of the leaf per dry mass [ $\Delta_m$ ]). (b) Equivalent predicted relationships involving only observed variables and a single latent ( $L$ ) in the form of a structural equation model.

nipulate each atom of element  $i$  in the newly expanded leaf be  $\delta_i$ . If the leaf requires a total mass of this element equal to  $E_i$  to construct the leaf until it becomes autotrophic, then the total cost to the plant with respect to this element is  $\delta_i E_i$  and the total construction cost of the leaf is  $\Delta = \sum \delta_i E_i$ . Since most carbon except for nonstructural carbohydrates is found in the cell wall, and construction costs do not include such nonstructural reserves, the total mass of carbon is approximately  $\bar{c}V_w$  where  $\bar{c}$  is the carbon mass per cell wall volume and is quite constant across species (Roderick et al. 1999b). The total mass of each of the mineral elements ( $e_i$ ) that are found primarily inside the cell is  $\bar{e}_i V_c$ , where  $\bar{e}_i$  is the mass of element  $i$  per cell volume. Separating elements that are located primarily in the cell (indexed by  $i$ ) or the cell wall (indexed by  $j$ ), the cost to construct the leaf is

$$\Delta = \sum_i \delta_i \bar{e}_i V_c + \sum_j \delta_j \bar{e}_j V_w.$$

Leaf construction cost per unit dry mass is therefore

$$\begin{aligned} \Delta_m &= \frac{\Delta}{M_c + M_w} \cong \frac{\Delta}{dV_w} \\ &\cong \sum_i \delta_i \bar{e}_i \frac{V_c}{dV_w} + \frac{1}{d} \sum_j \delta_j \bar{e}_j. \end{aligned}$$

Thus, the construction cost per unit dry mass of compounds within the cell will increase with the ratio of cell volume to cell wall volume, while the cost of compounds in the cell wall will be independent of this ratio (i.e.,  $V_c/V_w \rightarrow \Delta_m$ ).

Together, the variation in cell size and cell wall thickness and Kikuzawa's theory of optimal leaf longevity predict the trade-offs shown in Fig. 2a. The resulting structural equation model is shown in Fig. 2b. The dotted line will be absent if the concentration of nitrogen per cell volume is constant (or too small to be detected). Assuming the interspecific variation in  $\bar{n}$  to be negligible, we fit the GLOPNET data to Fig. 2b using ln-transformed variables and without the dotted line. Since we did not possess information on ( $V_c/V_w$ ), this variable is latent, and its scale was fixed by con-

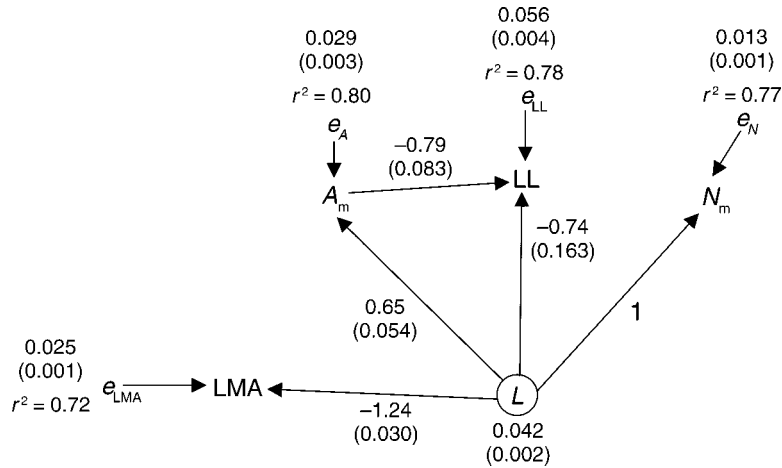


FIG. 3. The structural equation model of Fig. 2b including the fitted values. Path coefficients, the residual variances, the variance of the latent ( $L$ ), and the  $r^2$  values of the observed variables are shown, with the standard errors of estimates in parentheses.

straining the path coefficient ( $L \rightarrow N_m$ ) to unity as specified by the theory. The resulting model coefficients are shown in Fig. 3; this model fits the data remarkably well ( $\chi^2 = 0.766$ ,  $df = 1$ ,  $P = 0.38$ ) despite a very large sample size and the signs of all coefficients are in the predicted direction; note that this analysis is based on the full data set with missing values not only the 492 full observations. These coefficients represent the average responses over the full range of species and sites represented in the data set. Since regression analyses of bivariate pairs of these variables have detected site-specific differences in the slopes (Wright et al. 2005), it is likely that the path coefficients will also show such variation. The residual variances of all variables are significantly different from zero, indicating that there are additional unmeasured causes of each, and some of this residual variation might be due to site-specific differences.

These results provide support for the theoretical explanation developed above but do not unambiguously identify the latent variable as ( $V_c/V_w$ ); this would require direct measurement of this ratio. However, we did have a subset of 82 observations of Australian evergreen species for which we have measures of leaf water and dry mass. Assuming that leaf water mass is approximately equal to cell volume and that leaf dry mass is approximately equal cell wall mass (both approximations being poorer as leaves accumulate non-structural carbohydrates), the ratio of leaf water to leaf dry mass ( $W_m$ ) is approximately equal to ( $V_c/V_w$ ). We therefore tested the model shown in Fig. 2b using these new data plus the water mass:dry mass ratio as an additional indicator variable whose path coefficient was fixed at 1.0 since it should scale isomorphically with the latent variable, as described above; the path coefficient from the latent variable to  $N_m$  was also fixed to unity as done in Fig. 2b. The result is shown in Fig. 4. The model without the  $N_m \rightarrow LL$  path is rejected ( $\chi^2$

= 15.245,  $df = 4$ ,  $P = 0.004$ ), but the model including this path fits the data well ( $\chi^2 = 4.080$ ,  $df = 3$ ,  $P = 0.39$ ). Comparing Fig. 4b with Fig. 3, the main structural difference of this site-specific model is that leaf longevity primarily trades off with  $N_m$  rather than  $A_m$ . The strength of the correlation between  $W_m$  and the latent is lower than we had expected ( $r = 0.66$ ). This might reflect both that a nonnegligible proportion of the dry mass (e.g., nonstructural carbohydrates) was not in the cell wall, and also that a nonnegligible proportion of the leaf water can be found in the cell wall matrix (Berry and Roderick 2005). The rejection of the model in Fig. 4a in favor of the one in Fig. 4b might indicate either that the general explanation developed above requires revision or simply that these Australian species are unusual.

#### DISCUSSION

Despite a very large sample size and resulting statistical power to detect errors, we have produced a structural equation model that fits the data exceptionally well. This model suggests that the worldwide leaf economics spectrum has a surprisingly simple underlying structure that is generated by two general trade-offs. The first trade-off involves size–number relationships of living cells within the leaf (Pyankov et al. 1999, Niinemets 2001) and variation in cell wall thickness; this will be affected by the proportion of different types of tissues in the leaf. This first trade-off generates the broad interspecific coordination between  $A_m$ , LMA, and  $N_m$  and also determines the main interspecific differences in construction cost per dry mass of a leaf. This, in combination with the general tendency for photosynthetic rate to decrease with leaf age that is the basis for Kikuzawa’s model, generates the second trade-off between  $A_m$  and leaf longevity; namely that an increased  $A_m$  in a young leaf will decrease leaf longevity.

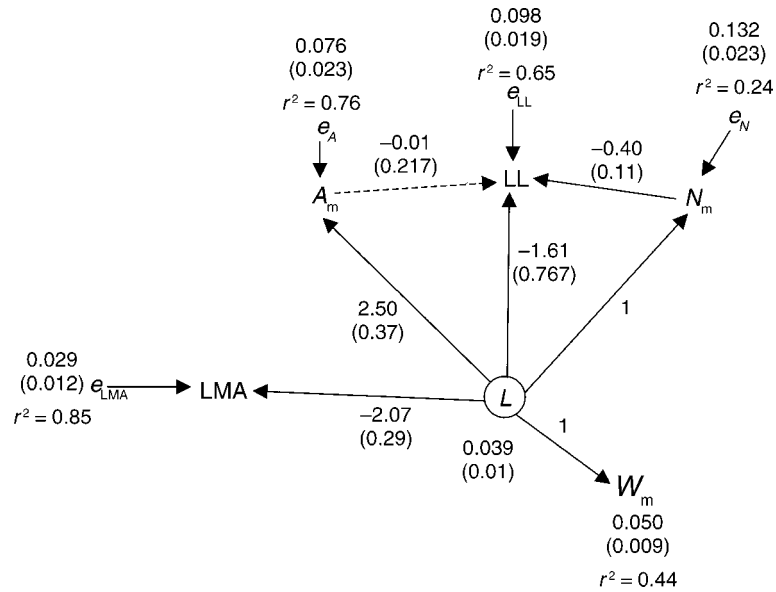


FIG. 4. The structural equation model of Fig. 2b, plus the mass of water per dry leaf mass ( $W_m$ ) including the fitted values. Path coefficients, residual variances, the variance of the latent ( $L$ ), and the  $r^2$  values of the observed variables are shown, with the standard errors of estimates in parentheses. Path coefficients not significantly different from zero are shown by broken lines.

It is perhaps surprising that models that posit direct effects between physiological variables such as net photosynthetic rate and leaf nitrogen content (cf. Fig. 1) were rejected in favor of a model (Fig. 3) that posits an indirect relationship mediated by size–number relationships of living cells within the leaf. An explanation is suggested by recognizing that these physiological processes occur at different scales (Marks and Lechowicz 2005). At the scale of a single chloroplast, the physiological mechanisms directly linking the photosynthetic enzymes and pigments to carbon fixation are well established. However, the GLOPNET variables are measured at the scale of an entire leaf; at this scale interspecific variation in the relationship between nitrogen amount and carbon fixation can arise both through interspecific differences in the functioning of a single chloroplast and through interspecific variation in the size and number of cells and chloroplasts in different leaves. Presumably, variation in these leaf-level variables is dominated by how differing numbers and volumes of cells and cell constituents are put together to form a leaf, while the physiological processes at the subcellular level are much more constant.

Our model does not require that all species have the same values for the path coefficients in all environments, only that the topological linkages between the variables (the way they link together) be the same. The estimated path coefficients are average values that capture the general tendency in the data; it is likely that separate intraspecific models would detect significant differences in the quantitative values of the path coefficients. Wright et al. (2005) detected significant, but quite small, levels of heterogeneity in slopes among

these variables between sites although much of the variability could be explained by differences in sample size. The degree to which species can escape from the two general trade-offs represented in our model is quantified by the residual variances. Since these residual variances were all significantly different from zero, this means that there are additional causes for each of these variables but that these additional causes are species and site specific. Understanding the origin of these residual variances is critical since, hidden within it, are the signals of small-scale differential adaptation to particular environments.

#### ACKNOWLEDGMENTS

This research was financially supported by the Natural Sciences and Engineering Research Council (NSERC) of Canada and by the National Science Foundation of the United States.

#### LITERATURE CITED

- Berry, S. L., and M. L. Roderick. 2005. Plant–water relations and the fibre saturation point. *New Phytologist* **168**:25–37.
- Desch, H. E. 1973. *Timber: its structure and properties*. Macmillan Press, London, UK.
- Field, C., and H. A. Mooney. 1986. The photosynthesis–nitrogen relationship in wild plants. Pages 25–55 in T. J. Givnish, editor. *On the economy of plant form and function*. Cambridge University Press, Cambridge, UK.
- Hikosaka, K. 2004. Interspecific difference in the photosynthesis–nitrogen relationship: patterns, physiological causes, and ecological importance. *Journal of Plant Research* **117**:481–494.
- Kikuzawa, K. 1991. A cost-benefit analysis of leaf habit and leaf longevity of trees and their geographical pattern. *American Naturalist* **138**:1250–1260.
- Little, R. J. A., and D. B. Rubin. 1987. *Statistical analysis with missing data*. Wiley and Sons, New York, New York, USA.

- Marks, C. O., and M. J. Lechowicz. 2006. A holistic tree seedling model for the investigation of functional trait diversity. *Ecological Modeling*, *in press*.
- Meziane, D., and B. Shipley. 2001. Direct and indirect relationships between specific leaf area, leaf nitrogen and leaf gas exchange. Effects of irradiance and nutrient supply. *Annals of Botany* **88**:915–927.
- Muthén, L. K., and B. O. Muthén. 1998–2001. *Mplus user's guide*. Second edition. Muthén and Muthén., Los Angeles, California, USA.
- Niinemets, U. 2001. Global-scale climatic controls of leaf dry mass per area, density, and thickness in trees and shrubs. *Ecology* **82**:453–469.
- Pearl, J. 2000. *Causality*. Cambridge University Press, Cambridge, UK.
- Pyankov, V., A. Kondratchuk, and B. Shipley. 1999. Leaf structure and specific leaf mass: the alpine desert plants of the Eastern Pamirs (Tadjikistan). *New Phytologist* **143**: 131–142.
- Pyke, K. A. 1999. Plastid division and development. *Plant Cell* **11**:549–556.
- Reich, P. B., M. B. Walters, and D. S. Ellsworth. 1997. From tropics to tundra: global convergence in plant functioning. *Proceedings of the National Academy of Sciences (USA)* **94**:13730–13734.
- Roderick, M. L., S. L. Berry, I. R. Noble, and G. D. Farquhar. 1999a. A theoretical approach to linking the composition and morphology with the function of leaves. *Functional Ecology* **13**:683–695.
- Roderick, M. L., S. L. Berry, A. R. Saunders, and I. R. Noble. 1999b. On the relationship between the composition, morphology and function of leaves. *Functional Ecology* **13**: 696–710.
- Shipley, B. 2000a. *Cause and correlation in biology: a user's guide to path analysis, structural equations, and causal inference*. Cambridge University Press, Cambridge, UK.
- Shipley, B. 2000b. A new inferential test for path models based on directed acyclic graphs. *Structural Equation Modeling* **7**:206–218.
- Shipley, B. 2003. Testing recursive path models with correlated errors using d-separation. *Structural Equation Modeling* **10**:214–221.
- Spirites, P., C. Glymour, and R. Scheines. 2000. *Causation, prediction, and search*. Second edition. MIT Press, Cambridge, Massachusetts, USA.
- Wishart, J. 1928. Sampling errors in the theory of two factors. *British Journal of Psychology* **19**:180–187.
- Wright, I. J., et al. 2005. Assessing the generality of global leaf trait relationships. *New Phytologist* **166**:485–496.
- Wright, I. J., et al. 2004. The worldwide leaf economics spectrum. *Nature* **428**:821–827.

#### APPENDIX

A description of the statistical analysis, including details of testing a structural equation model, identifying latent variables via vanishing tetrad differences, and the CI algorithm for exploratory path analysis (*Ecological Archives* E087-029-A1).